

Color-charge separation in trapped SU(3) fermionic atoms

Tobias Ulbricht¹, Rafael A. Molina², Ronny Thomale³, and Peter Schmitteckert⁴

¹*Institut für Theorie der Kondensierten Materie,*

Karlsruhe Institute of Technology, 76128 Karlsruhe, Germany

²*Instituto de Estructura de la Materia - CSIC, Serrano 123, 28006 Madrid, Spain*

³*Department of Physics, Princeton University, Princeton, NJ 08544, USA*

⁴*Institut für Nanotechnologie, Karlsruhe Institute of Technology, 76344 Eggenstein-Leopoldshafen, Germany*

Cold fermionic atoms with three different hyperfine states with SU(3) symmetry confined in one-dimensional optical lattices show color-charge separation, generalizing the conventional spin charge separation for interacting SU(2) fermions in one dimension. Through time-dependent DMRG simulations, we explore the features of this phenomenon for a generalized SU(3) Hubbard Hamiltonian. In our numerical simulations of finite size systems, we observe different velocities of the charge and color degrees of freedom when a Gaussian wave packet or a charge (color) density response to a local perturbation is evolved. The differences between attractive and repulsive interactions are explored and we note that neither a small anisotropy of the interaction, breaking the SU(3) symmetry, nor the filling impedes the basic observation of these effects.

PACS numbers: 71.10.Pm,05.30.Fk,03.75.Ss

One of the most intriguing effects of strong correlations in low-dimensional systems is the separation of charge and spin degrees of freedom. As a generic phenomenon, a quantum particle carrying spin and charge converts in separate spin (spinon) and charge (holon) excitations with generally different velocities. On a microscopic bare level, there are rare examples where this process can be exactly studied in terms of explicit (n species) spinon and holon wave functions, as is the case for the Kuramoto-Yokoyama model [1–4]. However, on a low-energy effective field theory level, spin-charge separation (SCS) explicitly manifests itself in all generic one-dimensional interacting systems belonging to the Luttinger liquid universality class, where spinons and holons are described by independent collective density-type excitations [5]. In spite of several attempts, the *direct* experimental observation of SCS has proved elusive [6–9]. So far, the best experimental evidence is provided by tunneling between quantum wires where interference effects relate to the existence of excitations with different velocities [10].

Since recently, one possible avenue for the observation and exploration of SCS are ultracold Bose or Fermi gases confined in optical lattices that have become an important instrument for investigating the physics of strong correlations. The great advantage of these systems is that the interaction parameters and dimensionality can be tuned with very high precision and control by means of an atomic Feshbach resonance or by changing the depth of the wells in an optical lattice [11]. One of the first achievements in this subject is the experimental observation of a superfluid to Mott insulator transition in a three-dimensional optical lattice with bosonic ⁸⁷Rb atoms [12]. Interesting experimental results have also been obtained for fermions, like the study of the molecule formation through the Feshbach resonance [13], the experimental observation of fermionic superfluidity [14], and

the observation of a Mott insulator in an optical lattice [15]. Several theoretical works have addressed the possibility of observing SCS in cold-fermionic gases [16–21] and in cold-bosonic gases [22] with two internal degrees of freedom. Thanks to the special properties of cold atomic systems these theoretical proposals could address previously unexplored features of SCS, like the problem of the breaking of SU(2) symmetry and SCS at high energies. In particular, higher spin fermions can be directly studied with cold atoms in more than two hyperfine states. This kind of systems could give rise to new phases in optical lattices due to the emergence of triplets and quartets (three or four fermion bound states), and other phenomena [23–29]. At least two alkali atoms ⁶Li and ⁴⁰K seem to be possible candidates for the experimental realization of an SU(3) fermionic lattice with attractive interactions [26]. In the case of ⁶Li the scattering lengths for the three possible channels of the three lowest lying hyperfine levels ($|F, m\rangle = |1/2, 1/2\rangle, |1/2, -1/2\rangle, \text{ and } |3/2, -3/2\rangle$) at large magnetic fields become similar for the three of them $a_s \approx -2500a_0$ [30]. Moreover, the realization of a stable and balanced three-component Fermi gas has been recently reported to potentially accomplish both an attractive and repulsive regime with approximate SU(3) symmetry [31, 32]. The scattering lengths of the different channels for the three lowest hyperfine states of ⁴⁰K near the Feshbach resonance was also measured and the possibility of trapping them optically was demonstrated [33].

It is the purpose of this work to use time-dependent Density Matrix Renormalization Group (td-DMRG) [34–38] simulations to study the phenomenology of CCS in lattice systems with three different kinds of fermions, where the color notation is inherited from the quark description of high energy SU(3) theories of quantum chromodynamics. As one of the significant quantities extractable from td-DMRG, the different color and charge

velocities are taken out from time-dependent simulations, and compared to a low energy bosonization approach.

The low energy physics of cold fermionic atoms with three different hyperfine states trapped in an optical lattice can be described by an SU(3) version of the Hubbard Hamiltonian,

$$H = -t \sum_{\langle ij \rangle, \alpha} \left(f_{i\alpha}^\dagger f_{j\alpha} + \text{h.c.} \right) + \sum_{i, \alpha \neq \beta} \frac{U_{\alpha\beta}}{2} n_{i\alpha} n_{i\beta}.$$

The sums α and β extend over the three colors red(r), green(g), and blue(b) corresponding to three different hyperfine states. The operators $f_{i\alpha}^\dagger$ and $f_{i\alpha}$ are the creation and destruction operators of an atom on site i with color α . We consider different values of the on-site interaction between the different color pairs $U_{\alpha\beta}$ to be able to include SU(3) symmetry breaking terms. The site label i goes from 0 to $L-1$, with L being the total number of lattice sites corresponding to the wells forming the optical lattice. For cold atoms, there is an additional harmonic confinement term that arises due to the Gaussian profile of the laser beams. If this trap potential is weak, we can assume to sit in the trap center where the confinement can be considered constant. Larger potentials could be taken into account, e.g. see [21]. In the subsequent calculations we will ignore the confinement. The hopping term can be controlled by varying the depth of the wells through the laser intensity. The optical lattice potential that each of the hyperfine states is affected by is very similar and the hopping rates can be considered to be equal for the three different colors. In the rest of the paper, all energies will be expressed in units of $t = 1$. The interaction strength in each channel is proportional to the corresponding s-wave scattering length $U_{\alpha\beta} = 4\pi\hbar^2 a_{\alpha\beta}/m$. The condition for the atoms to stay in the lowest band is that the s-wave scattering length must be smaller than the typical size of the wave function of an atom in one of the lattice wells [39]. In turn, this is easily fulfilled in the experiments, so we will neglect the population of higher bands. Spin-flipping rates are usually smaller than the escape rate of atoms from the optical lattices and can be neglected as well.

In the elementary linear bosonization approach, valid in the weak-coupling limit, the low-energy effective theory of the model can be expressed in terms of the collective fluctuations of the densities of the three spin species plus charge density. Introducing the three bosonic fields $\phi_\alpha(x)$, the density operators for each color can be written as

$$\rho_{i,\alpha} \approx \bar{\rho} + \frac{1}{\sqrt{\pi}} \partial_x \phi_\alpha(x) - \frac{1}{\pi} \sin \left[2k_F x + \sqrt{4\pi} \phi_\alpha(x) \right], \quad (1)$$

where k_F is the Fermi wave-vector and x corresponds to the lattice site. We can express the bosonized Hamiltonian in terms of the total density described by a bosonic

field

$$\Phi_{\text{ch}} = \frac{1}{\sqrt{3}} \sum_{\alpha} \phi_{\alpha}, \quad (2)$$

and the relative density described by two bosonic fields

$$\Phi_3 = \frac{1}{\sqrt{2}} (\phi_r - \phi_b) \quad (3)$$

$$\Phi_8 = \frac{1}{\sqrt{6}} (\phi_r + \phi_b - 2\phi_g). \quad (4)$$

The subindices were chosen to correspond to the SU(3) group Casimir operators J_3 and J_8 . For a SU(3) symmetric Hamiltonian, the model can be separated into two parts, charge and color, $H = H_{\text{ch}} + H_{\text{col}}$,

$$H_{\text{ch}} = \frac{v_{\text{ch}}}{2} \left[\frac{1}{K} (\partial_x \Phi_{\text{ch}})^2 + K (\partial_x \Theta_{\text{ch}})^2 \right], \quad (5)$$

where v_{ch} is the density velocity $v_{\text{ch}} = v_F/K$, $K = (1 + 2U/\pi v_F)^{-1/2}$ is the Luttinger liquid parameter, and Θ_{ch} is the conjugate field of the bosonic field Φ_{ch} , and

$$\begin{aligned} H_{\text{col}} = & \sum_{\mu=3,8} \left[\frac{v_F}{2} ((\partial_x \Phi_{\mu})^2 + (\partial_x \Theta_{\mu})^2) + \frac{U}{2\pi} (\partial_x \Phi_{\mu})^2 \right] \\ & + \frac{U}{2\pi^2} \cos \sqrt{2\pi} \Phi_3 \cos \sqrt{6\pi} \Phi_8 - \frac{U}{2\pi^2} \cos \sqrt{8\pi} \Phi_3. \end{aligned} \quad (6)$$

Similarly, the color velocity can be approximated as $v_{\text{col}} = v_F \sqrt{1 - U/(\pi v_F)}$. However, due to the non-linear cosine terms in (6), we do not expect a linear relation between distance and time for color excitations to hold for long times. If SU(3) symmetry is not strictly observed there appear mixing terms coupling density and color degrees of freedom. For example, if $U_{rg} = U_{rb} = U_1$ and $U_{gb} = U_2$ the mixing term can be written as $H_{\text{mix}} = \sqrt{2}(U_1 - U_2)/3\pi \cdot \partial_x \Phi_3 \partial_x \Phi_8$ [40]. A renormalization group analysis of this model can elucidate the low-energy properties of our system [40, 41]. The most important difference with respect to the SU(2) case is that when $U > 0$ but weak, umklapp processes present for commensurate fillings do not open a gap in the charge sector. We expect a phase transition between the MI and the LL at a finite value of U . In fact, with Monte-Carlo calculations, Assaraf *et al.* estimated the critical interaction scale at $U_{\text{cr}} = 2.2$ [40], while recent DMRG calculations suggest the critical point to be much closer to zero [42]. The cosine terms for the color Hamiltonian are irrelevant for repulsive, but relevant for attractive interaction and responsible of a gap opening in the color sector in the attractive case.

Let us now elaborate on how the CCS appears in real-time simulations. We study the time evolution of the Hamiltonian (1) with the td-DMRG algorithm [18, 35].

The number of states needed to keep sufficient accuracy during the time evolution was more than 7000. Such huge demands limited the system size we could simulate to $L = 18$ for periodic (PBC) and $L = 48$ for hard-wall boundary conditions (HWBC), which in total is settled in the range of present state of the art limits. For the small systems, the finite size effects are large. Comparable simulations on $SU(2)$ systems provided detailed knowledge about the finite size effects, so as that they are relatively independent on the interaction parameter. Comparison with exact results for $U = 0$ of the charge and color velocities provide us with approximations to the Luttinger liquid parameter.

We show snapshots of the time evolution for different interaction strengths in Fig. 1 for the system with $L = 18$ and PBC. We calculate the ground state $|\Psi_0\rangle$ of the $SU(3)$ Hamiltonian with $N = 27$ fermions and then put an extra (green) fermion with an initial wave packet in our system that travels to the right with a finite momentum centered around $k = 0.6\pi$

$$|\Psi^{+1}(t=0)\rangle = \sqrt{\frac{\pi}{2\sigma^2}} \sum_x e^{(ikx)} e^{-\frac{(x-x_0)^2}{2\sigma^2}} f_x^\dagger |\Psi_0\rangle, \quad (7)$$

where the width of the wave packet is chosen to be $\sigma = 1.5$. Choosing $N = 27$ leads to an average density of $\langle n \rangle = 1.5$ and an incommensurate filling of $\nu = 0.5$, the commensurate fillings being $\nu = 1/3, 2/3$. Time is always measured in inverse units of the hopping rate. The panels in the figure show the particle density $\langle n \rangle = \langle \Psi^{+1}(t) | \sum_\alpha f_\alpha^\dagger f_\alpha | \Psi^{+1}(t) \rangle$ and the corresponding densities of the color quantum numbers j^3 and j^8 relative to the uniform ground state density at initial and a finite time. We observe a slight dispersion effect due to the finite width of the wave-packet. Moreover, the velocity of the excitation is not exactly the velocity of a plane wave with momentum k . However, as relative velocity quantities are concerned, without interaction the charge density and color velocity are exactly the same (upper left panel). In Fig. 1, for the case $U = 1$, we start to see the separation of density and color degrees of freedom. The initial excitation separates and the color and charge density evolve with different velocities. The decay of the charge density excitation is more rapid for strong repulsive interaction as it is seen in the case $U = 5$, clearly indicating the opening of the charge gap. In similar ways, a gap in the color sector should open for attractive interaction, and spoil the color density evolution in that regime. However, in our example with $U = -1$, we can still observe rather clean and stable CCS, since, for our finite system, the arising gap in the color sector is too small to reasonably detect an enhanced color excitation decay. To extract color and charge velocities, we applied two different extraction methods. First, the velocity can be obtained dividing the number of sites traveled by the maximum of the density by the time. It is more accurate to fit a Gaussian on the density for every time step.

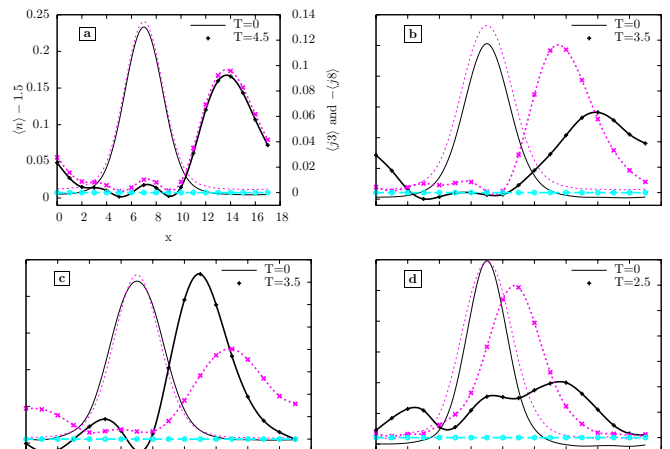


FIG. 1: (color online) Snapshots of the time evolution of an additional fermion for filling $\nu = 0.5$ and $U = 0$ (a), $U = +1$ (b), $U = -1$ (c) and $U = +5$ (d). The initial state is a Gaussian wave packet with average momentum $k = 0.6\pi$. In (b,c,d) the color density of quantum number j^8 (magenta) separates from the charge density (black), while j^3 (cyan) is constant by construction. Lines serve as guides to the eye.

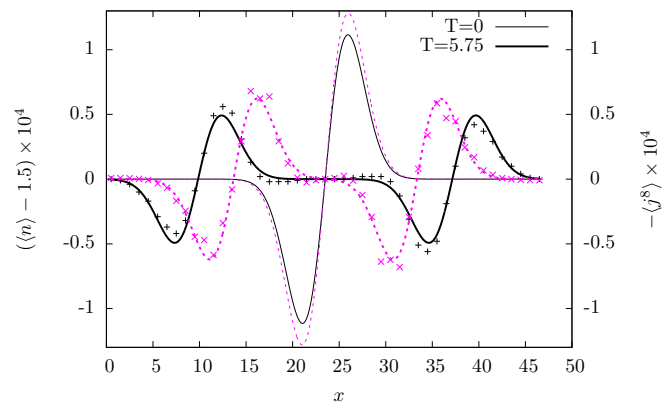


FIG. 2: (color online) Snapshots of a perturbation at time $T = 0$ (thin lines) and a finite time step (thick lines and data points). The dashed (solid) lines are fits to the color density of j^8 (charge density n) with the corresponding data points.

There is a short transient time at the beginning, followed by a plateau of constant velocity until the packet hits the boundary. We extracted the velocity of the packet when it passes the median between the initial position and the boundary and took a Gaussian averaged value around this position. As a second measure, for a definite plateau of constant velocity, we used a $L = 48$ sites system with HWBCs and replaced the incident electron by an initial, small potential perturbation. The time development of this method differs mainly by the implicit stimulation of excited states around both Fermi points leading to symmetric peaks running in both directions and increasing the transient time at the start. Fig. 2 shows snapshots of the initial and a finite time step for $U = 1.5$, where the perturbation was taken to be the derivative of a Gaus-

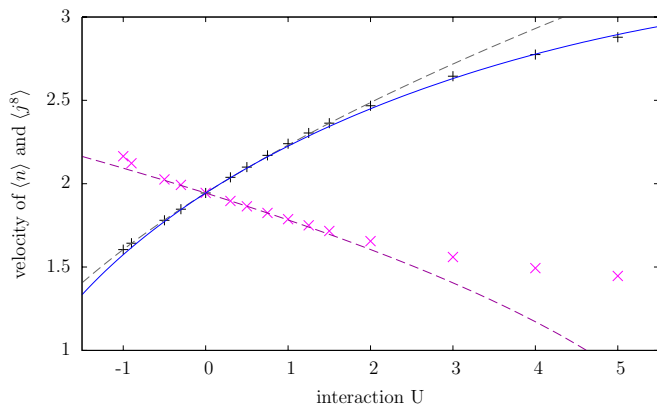


FIG. 3: (color online) Velocity $v(U)$ of an initial Gaussian perturbation. Results of our td-DMRG simulations for both charge density (+) and color density (x). The dashed lines represent bosonization results, scaled to match the DMRG velocity at $U = 0$. The solid line is a fit on a next-to linear dependency in U .

sian and this function was fitted on the two propagating wave packets. We find that both methods provide similar results, while the latter proved to be a considerable improvement in precision and is put forward by us as a general preferable method to extract velocities from td-DMRG.

Finally, the extracted velocities are shown as a function of the uniform interaction in Fig. 3. On top of the data, we show the expected relation for $v_{\text{col}}(U), v_{\text{ch}}(U)$ from bosonization, scaled to match the free fermion velocity. This *a priori* renormalization covers all direct effects that lead to deviations of the Fermi velocity due to finite width or the central momentum k_0 of the excitation and the finite size dispersion. Even for $|U|$ up to 1, the agreement between the bosonization estimate and the numerical data is found to be excellent (dashed lines in Fig. 3). Beyond, the limits of the low energy expansion are apparently reached. However, upon extending the velocity expansion to higher order in U , e.g. $v_{\text{ch}} = v_F \sqrt{1 + 2U/(\pi v_F) + aU^2}$, the fit already covers the complete computed range in U (solid line in Fig. 3) and the parameter $a = -0.017$ has the same order and sign as the fit by Assaraf *et al.* [40] who chose a different filling in their Monte-Carlo simulations.

A possible candidate for realizing the trionic phase ($U < 0$) is ${}^6\text{Li}$ for which the magnetic field dependence of the three scattering lengths has been measured [30]. The attractive U interaction for magnetic fields around 1000 G can be estimated as $U_{rg} = U_0$, $U_{rb} = 1.23U_0$, and $U_{gb} = 1.06U_0$, due to the ratios in the s -wave scattering rate in each channel [30]. It is important to consider whether these anisotropies infringe on the validity of the effects observed above. In bosonization theory, anisotropy introduces new terms that couple the charge and color degrees of freedom so we would expect

that high anisotropies totally destroy charge-color separation [41]. However, small and experimentally accessible anisotropies turn out to be not decisively important. We have checked that the separation effect of color and charge densities is still visible in the simulations without much change. Even for the special cases of commensurate fillings where a stronger sensitivity on the color anisotropy may have been suspected, the qualitative behavior persists.

In summary, we have performed td-DMRG simulations of cold fermionic atoms with three hyperfine states trapped in an optical lattice. Our simulations allowed us to observe the color-charge separation in $\text{SU}(3)$ fermionic systems in a generic non-commensurate case. We have obtained the charge and color velocities as a function of the interaction from the real-time simulations both for the attractive and repulsive case. Once we take into account finite size effects by renormalizing the non-interacting velocities, our results at weak coupling are in good agreement with bosonization calculations.

The authors acknowledge discussions with Philippe Lecheminant and Stephan Rachel. RAM is supported in part by Spanish Government grant No. FIS2009-07277, RT by a Feodor Lynen Fellowship of the Humboldt Foundation. We acknowledge the support by the Center for Functional Nanostructures (CFN), project B2.10.

-
- [1] B. A. Bernevig, D. Giuliano, and R. B. Laughlin, *Phys. Rev. B* **65**, 195112 (2002).
 - [2] R. Thomale, D. Schuricht, and M. Greiter, *Phys. Rev. B* **74**, 024423 (2006).
 - [3] R. Thomale, D. Schuricht, and M. Greiter, *Phys. Rev. B* **75**, 024405 (2007).
 - [4] Y. Kuramoto and H. Yokoyama, *Phys. Rev. Lett.* **67**, 1338 (1991).
 - [5] T. Giamarchi, *Quantum Physics in One Dimension, International Series of monographs on physics*, Oxford University Press (2004).
 - [6] M. Bockrath *et al.*, *Nature (London)* **397**, 598 (1999).
 - [7] P. Segovia, D. Purdie, M. Hengsberger, and Y. Baer, *Nature* **402**, 504 (1999).
 - [8] R. Losio *et al.*, *Phys. Rev. Lett.* **86**, 4632 (2001).
 - [9] T. Lorenz *et al.*, *Nature* **418**, 614 (2002).
 - [10] O. M. Auslaender *et al.*, *Science* **308**, 88 (2005).
 - [11] M. Lewenstein *et al.*, *Adv. Phys.* **56**, 243 (2007).
 - [12] M. Greiner *et al.*, *Nature* **415**, 39 (2002).
 - [13] T. Stöferle *et al.*, *Phys. Rev. Lett.* **96**, 030401 (2006).
 - [14] J. K. Chin *et al.*, *Nature* **443**, 961 (2008).
 - [15] R. Jördens *et al.*, *Nature* **455**, 204 (2008).
 - [16] C. Kollath, U. Schollwöck, and W. Zwerger, *Phys. Rev. Lett.* **95**, 176401 (2005).
 - [17] C. Kollath and U. Schollwöck, *New J. Phys.* **8**, 220 (2006).
 - [18] T. Ulbricht and P. Schmitteckert, *EPL* **86**, 57006 (2009).
 - [19] P. Schmitteckert and G. Schneider, in *High Performance Computing in Science and Engineering '06*, ed. by W. E. Nagel, W. Jäger, M. Resch, Springer, Berlin, 113 (2006).

- [20] P. Schmitteckert, in High Performance Computing in Science and Engineering '07, ed. by W. E. Nagel, D. B. Kröner, M. Resch, Springer, Berlin, 99 (2007).
- [21] T. Ulbricht and P. Schmitteckert, EPL, (accepted for publication)(2010) .
- [22] A. Kleine *et al.*, Phys. Rev. A **77**, 013607 (2008).
- [23] C. Wu, Phys. Rev. Lett. **95**, 266404 (2005).
- [24] P. Lecheminant, E. Boulat, and P. Azaria, Phys. Rev. Lett. **95**, 240402 (2005).
- [25] H. Kamei and K. Miyake, J. Phys. Soc. Jpn. **74**, 1911 (2005).
- [26] A. Rapp, G. Zaránd, C. Honerkamp, and W. Hofstetter, Physical Review Letters **98**, 160405 (2007).
- [27] C. Honerkamp and W. Hofstetter, Phys. Rev. Lett. **92**, 170403 (2004).
- [28] A. V. Gorshkov *et al.*, arXiv:0905.2610, (unpublished).
- [29] S. Rachel *et al.*, Phys. Rev. B **80**, 180420(R) (2009).
- [30] M. Bartenstein *et al.*, Phys. Rev. Lett. **94**, 103201 (2005).
- [31] T. B. Ottenstein *et al.*, Phys. Rev. Lett. **101**, 203202 (2008).
- [32] J. H. Huckans *et al.*, Phys. Rev. Lett. **102**, 165302 (2009).
- [33] C. A. Regal, Ph.D. thesis, .
- [34] S. R. White, Phys. Rev. Lett. **69**, 2863 (1992).
- [35] P. Schmitteckert, Phys. Rev. B **70**, 121302(R) (2004).
- [36] A. J. Daley, C. Kollath, U. Schollwöck, and G. Vidal, J. Stat. Mech. **2004**, P04005 (2004).
- [37] S. R. White and A. E. Feiguin, Phys. Rev. Lett. **93**, 076401 (2004).
- [38] U. Schollwöck, Rev. Mod. Phys. **77**, 259 (2005).
- [39] D. Jaksch *et al.*, Phys. Rev. Lett. **81**, 3108 (1998).
- [40] R. Assaraf, P. Azaria, M. Caffarel, and P. Lecheminant, Phys. Rev. B **60**, 2299 (1999).
- [41] P. Azaria, S. Capponi, and P. Lecheminant, Phys. Rev. A **80**, 041604(R) (2009).
- [42] K. Buchta, O. Legeza, E. Szirmai, and J. Sólyom, Phys. Rev. B **75**, 155108(R) (2007).